1
2 **Pedogenesis and clay mineralogy of a climolithotoposequence in Jazmurian Watershed, central Iran**

3 **Saleh Sanjari[1], and Mohammad Hady Farpoor[1]***

4 **Abstract**

5 Topography, parent material, and climate are critical factors influencing pedogenesis and the clay
6 mineralogy of soils. There is a paucity of data regarding the soils and sediments of the Jazmurian
7 Watershed in south-central Iran. This study selected various landforms, including rock and mantled
8 pediments, alluvial fans, piedmont plains, lowlands, and playa, characterized by igneous and
9 sedimentary parent materials and situated within aquic, xeric, and aridic soil moisture regimes, to
10 investigate soil genesis and clay mineralogy in the region. The findings indicated that the most
11 significant soil development occurred on rock and mantled pediments, as well as on older alluvial
12 fan sediments, in contrast to the less developed soils found on younger alluvial fan deposits. The
13 clay minerals identified through X-ray diffraction (XRD) analyses included smectite, illite,
14 chlorite, palygorskite, and kaolinite. The presence of palygorskite in the sedimentary soils was
15 attributed to inheritance from the parent material, while in soils derived from igneous parent
16 material, palygorskite was formed through pedogenic processes. Pedogenic features associated
17 with calcium carbonate, such as coatings, infillings, and nodules, as well as clay coatings and
18 infillings, were observed in both aridic and xeric soil moisture regimes. The occurrence of clay
19 pedogenic features in the arid regions of the watershed may suggest a historical paleoclimate with
20 greater moisture availability. Conversely, lenticular shapes, interlocked plates, and gypsum
21 infillings were exclusively noted in the arid regions and lower elevations of the watershed,
22 reflecting the current arid climate. The study established a strong correlation between soil
23 formation and the factors of climate, parent material, and relief within the area.

24 **Keywords:** Central Iran, Geomorphic surface, Paleoclimate, Paleosols, Soil evolution.

25
26 **1. Introduction**

27 Soil formation and evolution influenced by soil-forming factors have been the focus of many
28 pieces of research (Badia et al., 2020; Owliaie et al., 2018; Wilson et al., 2017; Yousefifard et al.,

---

[1] Department of Soil Science, Faculty of Agriculture, Shahid Bahonar University of Kerman, P.O. Box: 76169-14111, Kerman, Islamic Republic of Iran.
* Corresponding author; e-mail: farpoor@uk.ac.ir

29 2015, Farpoor et al., 2012, Moazallahi and Farpoor, 2012; Saez et al., 2003). Soil genesis related

30 to geomorphology helps better understanding of soil forming factors and processes (Moghbeli et

31 al., 2019; Sanjari et al., 2011). Owliaie et al. (2018) reported the impact of parent material and

32 geomorphic position on physicochemical properties, clay mineralogy, and micromorphology of

33 soils, south western Iran.

34 Lithology, together with other soil forming factors is reported as a major factor affecting

35 pedogenesis (Wilson et al., 2017). Soil characteristics in northwest Iran affected by volcanic and

36 plutonic rocks were studied by Yousefifard et al. (2015). They found more evolution in soils

37 derived from volcanic rocks compared to plutonic ones. Soil properties and evolution were mainly

38 affected by particle size and mineralogy of parent material in soils of arid Kapehdagh Basin,

39 northeast Iran, which is an emphasis on the relationship between soil and parent material in that

40 area.

41 Climate has a major role on the weathering processes of parent material. Climatic variations

42 influence on the type and the rate of soil forming processes which in turn affect physicochemical

43 properties and clay mineralogy of soils (Phillips et al., 2008). Weathering is highly related to the

44 climate and trioctahedral minerals such as mica and chlorite may transform to dioctahedral smectite

45 due to the high rate of weathering (Egli et al., 2008). Soil evolution in Nevada was affected by

46 weathering rate and moisture regime (Elliot and Dorhan, 2009).

47 Soil minerals could be used to understand soil genesis (Graham and O'Geen, 2010), manage arid

48 and wet land soils (O'Geen et al., 2008), and interpret paleo environmental conditions (Sanjari et

49 al., 2012; Monafi, 2010; Khormali and Abtahi, 2003). Clay mineralogy of soils in Jiroft area,

50 central Iran showed that due to high water table, palygorskite stability decreased and smectite

51 dominated in soils from mantled pediment toward alluvial plain (Sanjari et al., 2011). In a soil

52 geomorphology study of the southern parts of central Iran, Sarmast et al. (2017) reported chlorite,

53 smectite, illite, palygorskite, and kaolinite clay minerals on different geomorphic positions.

54 Micromorphology is a useful complementary tool for soil morphology and evolution studies and

55 seems necessary to better classify and manage soils of an area (Stoops, 2003). In a soil

56 geomorphology study of Sirjan Playa, central Iran, Farpoor et al. (2012) reported calcite coatings

57 and infillings in pediments, but lenticular shape and interlocked plates of gypsum in piedmont plain

58 and playa landforms. Clay coating and infilling in the piedmont plain was attributed to the more

59 available humidity of the climate in the past by the same researchers. Soil micromorphology related

60 to geomorphic position in central Iranian soils was studied by Sarmast et al. (2019). They reported

61 clay (coating), calcite (nodule, coating, quazicoating, and infilling), anhydrite (nodule), gypsum

62 (lenticular, vermiform, and interlocked plates), and halite (coating) pedo-features in the area under

63 study.

64 Sixty watersheds were investigated in a study conducted by Krinsley (1970) in central Iranian

65 plateau and Jazmurian is among the most widespread playas reported in that report. Limited data

66 about soils and environmental factors in this playa are available. The only published report dates

67 back to the study on sediments of the area related to geomorphic positions using aerial photo

68 interpretations and limited field studies (Krinsley, 1970). Since climate, parent material, and

69 geomorphic position are hypothesized to affect soil genesis and evolution on one hand, and limited

70 data on soils of the study area are reported from the other hand, the present research was conducted

71 with the following objectives: to study 1) physicochemical soil properties, clay mineralogy, and

72 soil micromorphology in soils of the area, 2) the origin and distribution of clay minerals related to

73 the variation of soil forming factors, 3) soil development along a climotopolithosequence.

74

75 **2. Materials and methods**

76 **2.1. Study area**

77 Jazmurian Watershed as a part of central Iran, Makran, and southeast Iran zones located in

78 Kerman and Sistan-Baluchestan Provinces (56° E to 62° E and 26° N to 30° N) was selected as the

79 study area (Fig. 1). The maximum elevation in the area is 4400 m above sea level (asl) for the Shah

80 Mountain, Rabor area and the minimum elevation is only 360 m (asl) at Jazmurian Playa.   Two

81 main rivers including non-saline Halilrood which heads from Kerman Province elevations (north

82 of the watershed) and saline Bampoor which heads from Iranshahr elevations (east side of the

83 watershed), both end to central lake of Jazmurian Playa (Fig. 1). Jazmurian Playa is a depression

84 of Late Pliocene Era (Namaki 2003). Miocene faulted rocks and evaporites of Upper Red

85 Formations are at the east boundary of the watershed. Jebalbarez igneous mountain (granite, diorite,

86 and andesite) is located at north. Intrusive and external igneous rocks are reported at the west and

87 southeast sides of the area and the Beshagard Paleocene and Cretaceous Ophiolite Mountains

88 together with Mokran colored Melange which separate the watershed from Oman Sea are located

89 at the south (Mohammadi, 2011). Soil mean temperature varies from 13.1 °C in Rabor and Hanza

90 (Mesic soil temperature regime) to 28.9 °C in Iranshahr and Dalgan areas (Hyperthermic soil

91   temperature regime). Mean Annual precipitation also varies from 287 mm in Rabor and Hanza

92   (Xeric moisture regime) to 82 mm in Roodbar Jonoub areas (Aridic soil moisture regime).
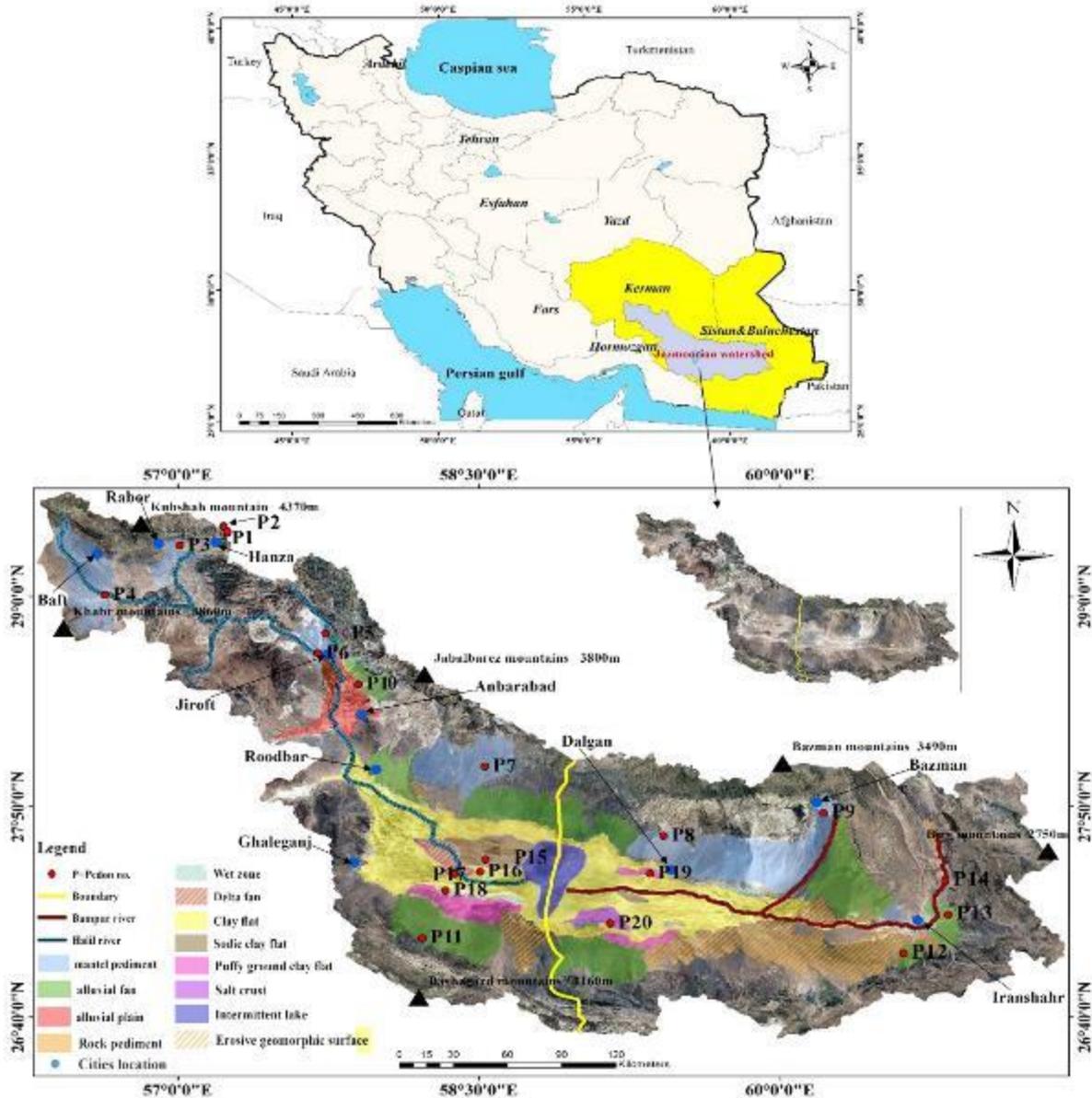
93

94   **Fig. 1.** The study area, geomorphology map showing location of representative pedons.

95   **2.2. Field studies**

96   Alluvial fan, rock and mantled pediments, Piedmont plain, playa, and lowland were among

97   dominant landforms studied after detailed field and aerial photo observations (Fig. 1). Playa was

98   also divided to clay flat, sodic clay flat, puffy ground clay flat, salt crust, wet zone, fan delta, and

99   lake geomorphic surfaces. Considering variations in elevation, soil moisture and temperature

100   regimes, and parent material, one representative pedon on each geomorphic surface (total of 20

101   pedons) were selected, described (Schoeneberger et al., 2012), and sampled. Fig. 1 shows the study

102   area and the location of representative pedons.

103   Various soil moisture regimes included; xeric (pedons 1 and 3), aquic (pedons 2, 18) and aridic

104   (other pedons) and temperature regimes included mesic (pedons 1, 3 and 4), thermic (9),

105   hyperthermic (other pedons) related to elevation variations and the vast extent of the area were

106   found (Banaie, 1998).

107

108   **2.3. Laboratory investigations**

109   After sampling, air-dried ground soil samples passed through a 2 mm sieve and the volumetric

110   percentage of coarse fragments was determined. Particle size distribution was investigated using

111   pipet method (Gee and Bauder, 1986). Jenway pH and EC meters were used to determine the pH

112   of saturated paste and the EC of saturated extract, respectively. The sum of gypsum and anhydrite

113   was analyzed using acetone precipitation (Nelson, 1982). Gypsum was investigated using the Oven

114   method (Artieda et al., 2006). Anhydrite was calculated by the subtraction of gypsum from

115   gypsum+anhydrire (Wilson et al. 2013). Back titration of excess NaOH by HCl was used for

116   equivalent calcium carbonate determination (Nelson, 1982). Wet oxidation using potassium

117   dichromate (Nelson and Sommers, 1982) was used for organic carbon determination. Substitution

118   of sodium acetate by ammonium acetate pH=7 was the basis for cation exchange capacity (CEC)

119   determinations (Bower and Hatcher, 1966).

120

121   **Micromorphological study**

122   Undisturbed soil samples were impregnated using a Vestapol resin with acetaeric acid as the

123   hardener and cobalt acetate as the catalyst for micromorphological studies, under vacuum. A BK-

124   POL petrography microscope in plain (PPL) and crossed (XPL) polarized lights was used for thin

125   section observations and interpretations performed by the Stoops (2003) guideline.

126

127   **Clay mineralogy**

128   Soil samples were prepared (Jackson, 1975; Kittrick and Hope, 1963) for XRD analysis and four

129   treatments including Mg-saturated, Mg-saturated and treated by ethylene glycol, K-saturated, and

130   K-saturated and heated up to 550 ºC performed on each sample. A Broker DH8 Advance

131   diffractometer with Cu as the target at 40 kv and 30 mA with the scan speed of 0.02 degree per

132 second was used for XRD analyses. The area under first order peaks of Mg saturated-treated by

133 ethylene glycol was used as the reference for semi-quantitative clay mineralogy (Jones et al., 1954).

134 Besides, several bulk soil samples were mounted on Al stubs by a carbon glue, coated with gold,

135 and observed by scanning electron microscope (XL 30 ESEM Philips) as a complementary to clay

136 mineralogy investigations.

137
138 **3. Results and discussion**

139 Table 1 shows selected physiochemical soil properties and soil classifications based on Soil

140 Taxonomy (Soil Survey Staff, 2022) system.

141
142 **3.1. Piedmont Plain**

143 Pedon 1 on this geomorphic position is about 3620 m above sea level (asl) with a xeric moisture

144 regime affected by diorite derived parent material (Fig. 1). Mollic and cambic horizons were

145 determined through field studies, but no calcic or gypsic horizon was found. Gleyic condition

146 caused by textural differentiation was the reason an Oxyaquic Haploxeroll to be formed.

147 Smectite, illite, chlorite, and kaolinite clay minerals were found in the Bw1 horizon and R layer

148 (Table 2) which are accounted as a proof of the inheritance origin of minerals from parent material

149 (Yousefifard et al., 2015). Palygorskite was also found in the Bw1 horizon (Table 2, Fig. 3a). Since

150 palygorskite was neither present in the parent material (Fig. 3b), nor were the environmental

151 conditions in this pedon suitable for its formation due to relatively high precipitation, the detrital

152 origin (aeolian source) in this geomorphic surface could be a plausible reason for palygorskite as

153 also supported by other researchers (Sarmast et al., 2017; Singer, 1989).

154
155 **3.2. Lowland**

156 This geomorphic position with the elevation of 3570 m asl and an aquic soil moisture regime was

157 also affected by diorite parent rock (Fig. 1). Pedon 2 on this surface with Histic and Cambic

158 horizons showed gleyic properties. Water logging together with a cold climate inhibited organic

159 matter decomposition that is why about 16% organic carbon with an intermediate decomposition

160 in this pedon was accumulated and caused Histic Humaquepts to be formed.

161 Illite and kaolinite were the only clay minerals formed in this pedon (Table 2, Fig.3c).

162 Transformation of smectite to kaolinite due to high precipitation rate and low pH (Table 1) in this

163 pedon could not be neglected. This could be the reason why the highest kaolinite content was found

164   in this pedon. On the other hand, lack of palygorskite is attributed to high weathering rate and the

165   mineralogy of parent material which lacks palygorskite (Moazallahi and Farpoor, 2012).

166   Transformation of palygorskite to smectite is reported to take place at the annual rainfalls more

167   than 300 mm (Paquet and Millot, 1972) as a support.

168   Pedons 1 and 2 have the same parent material but different geomorphology and soil moisture

169   conditions. Since the soils formed on the two mentioned locations are different (Haplustolls vs.

170   Humaquepts), it is clear that climate (xeric vs. aridic) and topography (piedmont plain vs. lowland)

171   played an important role on soil genesis and development in the area compared to parent material

172   (both diorite).

173   **Table 1.** Selected physical and chemical properties of studied pedons.

Horizon	Depth (Cm)	Sand (%)	Silt (%)	Clay (%)	RF (%)	pH	ECe (dS m^{-1})	CCE (%)	Gypsum (%)	Anhydrite (%)	OC (%)	SAR (mmol L^{-1})$^{0.5}$
Pedon 1, Piedmont plain, 3620 m a.s.l., Diorite, USDA: Oxyaquic Haploxerolls												
A	0-20	15.1	46.6	38.3	2	6.5	1.2	2.0	ng	ng	3.5	1.1
Bw1	20-45	19.1	50.6	30.3	7	6.0	0.7	1.0	ng	ng	1.2	1.6
Bw2	45-80	27.1	48.6	24.3	18	6.4	0.5	0.7	ng	ng	0.7	1.4
Bg	80-100	11.1	51.6	37.3	23	6.5	0.4	1.7	ng	ng	0.9	1.4
C	100-140	37.1	44.6	18.3	46	6.6	0.5	1.2	ng	ng	0.5	1.6
R	>140	-	-	-	-	-	-	-	-	-	-	-
Pedon 2, Low land, 3570 m a.s.l., Diorite, USDA: Histic Humaquepts												
Oe	0-15	25.1	51.1	23.8	-	5.6	1.5	1.0	ng	ng	16.0	1.0
A	15-30	45.1	24.6	30.3	23	5.8	0.8	1.0	ng	ng	2.3	1.1
Bg1	30-65	53.1	16.6	30.3	27	5.8	0.5	0.5	ng	ng	1.4	1.4
Bg2	65-110	65.1	14.6	20.3	18	5.1	0.6	0.75	ng	ng	0.5	2.0
Pedon 3, Mantled pediment, 2247 m a.s.l., Andesite, USDA: Calcic Haploxeralfs												
A	0-13	39.1	39.3	21.6	6	7.2	1.4	8.5	ng	ng	0.5	1.5
Btk	13-45	35.1	37.3	27.6	34	7.9	0.9	26.2	ng	ng	0.6	2.0
Ck	45-85	71.1	13.3	15.6	58	7.8	0.8	17.7	ng	ng	0.3	2.3
C	85-105	77.1	9.3	13.6	66	7.6	0.6	14.0	ng	ng	0.2	2.4
2Btk	105-145	7.1	65.3	27.6	-	7.7	0.6	15.0	ng	ng	0.1	2.5
2Bk1	145-175	23.1	58.6	18.3	-	8.0	0.7	24.0	ng	ng	0.1	3.0
2Bk2	175-215	11.1	68.6	20.3	-	7.9	0.7	44.2	ng	ng	0.1	3.4
Pedon 4, Mantled pediment, 1977 m a.s.l., Limestone, USDA: Typic Natrargids												
A	0-5	37.1	41.3	21.6	1	8.0	0.5	26.5	ng	ng	0.4	0.5
Btk1	5-35	23.1	39.3	37.6	-	8.3	1.2	28.7	ng	ng	0.3	6.2
Btk2	35-72	25.1	35.3	39.6	-	7.8	5.6	28.2	ng	ng	0.3	11.9
C	72-78	57.1	17.3	25.6	19	7.8	5.5	19.5	ng	ng	0.1	12.9
2Btnk	78-100	43.1	27.3	29.6	-	7.9	4.7	22.2	ng	ng	0.1	15.2
2Btnkk1	100-135	1.1	53.3	45.6	-	8.3	2.8	51.2	ng	ng	0.1	15.5
2Btnkk2	135-185	0	58.4	41.6	-	8.2	3.3	50.7	ng	ng	0.1	13.8
2Ckk	>185	0	89.4	10.6	-	8.0	3.6	88.9	ng	ng	ng	12.6
Pedon 5, Mantled pediment, 897 m a.s.l., Diorite, USDA: Calcic Argigypsids												
A	0-20	75.7	12.9	11.4	43	7.6	2.7	15.5	ng	ng	0.2	1.0
Btk	20-55	70.7	14.9	14.4	34	8.0	1.1	16.5	0.7	ng	0.2	1.4
By	55-85	89.7	1.9	8.4	69	8.0	1.3	14.5	5.2	ng	0.2	2.4
C	85-135	90.7	2.9	6.4	60	8.2	1.4	10.0	5.5	ng	0.3	1.2
Pedon 6, Mantled pediment, 860 m a.s.l., Diorite, USDA: Typic Natrargids												
A	0-20	51.4	17.0	31.6	5	7.6	1.6	20.0	ng	ng	ng	4.7

Horizon	Depth (Cm)	Sand (%)	Silt (%)	Clay (%)	RF (%)	pH	ECe (dS m^{-1})	CCE (%)	Gypsum (%)	Anhydrite (%)	OC (%)	SAR (mmol L^{-1})$^{0.5}$
Btn1	20-65	41.4	16.0	42.6	-	7.6	8.2	19.5	ng	ng	0.1	16.5
Btn2	65-80	40.4	18.0	41.6	-	7.5	5.9	19.7	ng	ng	0.1	14.1
Btn3	80-125	39.4	20.0	40.6	-	7.6	5.2	20.5	ng	ng	0.1	13.3
C	125-140	79.4	9.0	11.6	84	7.8	2.4	20.2	ng	ng	0.1	5.7
2Btk	140-170	61.4	15.0	23.6	52	7.8	2.0	20.5	ng	ng	0.1	5.1
2Ck	170-200	85.4	6.0	8.6	72	7.9	1.3	21.2	ng	ng	0.1	2.5

Pedon 7, Mantled pediment, 615 m a.s.l., Diorite, USDA: Typic Haplogypsids

Horizon	Depth (Cm)	Sand (%)	Silt (%)	Clay (%)	RF (%)	pH	ECe (dS m^{-1})	CCE (%)	Gypsum (%)	Anhydrite (%)	OC (%)	SAR (mmol L^{-1})$^{0.5}$
A	0-10	67.1	16.6	16.3	55	7.4	8.0	11.7	0.6	3.8	0.1	4.3
By1	10-25	79.1	10.6	10.3	49	7.5	4.8	8.7	0.8	13.4	0.1	3.0
By2	25-50	81.8	6.6	11.6	45	7.6	2.9	4.2	23.0	2.7	ng	1.1
By3	50-80	81.8	8.6	9.6	56	7.6	2.9	3.5	14.1	ng	0.1	1.3
By4	80-120	79.8	6.6	13.6	56	7.7	2.9	3.0	14.0	ng	0.1	1.3
Bym	120-150	81.8	4.6	13.6	76	7.4	3.0	4.2	17.3	ng	ng	1.4
Bty	150-180	73.8	4.6	21.6	54	7.6	3.0	3.2	5.5	ng	0.1	1.5

Pedon 8, Mantled pediment, 490 m a.s.l., Andesite, USDA: Petrogypsic Haplosalids

Horizon	Depth (Cm)	Sand (%)	Silt (%)	Clay (%)	RF (%)	pH	ECe (dS m^{-1})	CCE (%)	Gypsum (%)	Anhydrite (%)	OC (%)	SAR (mmol L^{-1})$^{0.5}$
A	0-10	55.8	33.3	10.9	21	7.4	43.5	37.7	0.7	ng	0.4	53.0
Bkyz1	10-35	47.8	41.3	10.9	24	7.1	140.5	27.2	2.0	17.4	0.4	64.5
Bkyz2	35-65	61.8	28.6	9.6	63	7.3	84.7	24.5	24.2	2.5	0.1	59.4
Bym	65-110	53.8	32.6	13.6	61	7.3	99.6	34.0	15.8	2.3	0.2	66.8
Bkyz	110-160	51.8	38.6	9.6	67	7.6	96.1	47.5	7.5	0.8	0.8	92.4
Ck	160-190	69.8	20.6	9.6	67	7.6	9.4	45.0	0.1	ng	0.1	7.0

Pedon 9, Mantled pediment, 860 m a.s.l., Diorite, USDA: Typic Natrigypsids

Horizon	Depth (Cm)	Sand (%)	Silt (%)	Clay (%)	RF (%)	pH	ECe (dS m^{-1})	CCE (%)	Gypsum (%)	Anhydrite (%)	OC (%)	SAR (mmol L^{-1})$^{0.5}$
A	0-15	79.1	8.6	12.3	22	7.7	5.6	8.2	ng	ng	0.1	14.4
Bk	15-40	76.5	15.3	8.2	26	7.4	9.2	16.0	ng	ng	0.1	11.4
Btk	40-55	56.5	25.3	18.2	35	7.3	25.5	16.2	0.6	ng	0.1	12.5
Btky	55-80	64.5	15.3	20.2	27	7.6	20.9	16.7	7.4	ng	0.1	11.3
Btnky1	80-140	66.5	15.3	18.2	34	7.6	19.8	15.5	5.8	ng	0.1	22.2
Btnky2	140-175	52.5	29.3	18.2	53	7.5	22.3	17.5	6.3	ng	ng	21.3

Pedon 10, Alluvial fan, 700 m a.s.l., young alluvial fan (Granite), USDA: Typic Torrifluvents

Horizon	Depth (Cm)	Sand (%)	Silt (%)	Clay (%)	RF (%)	pH	ECe (dS m^{-1})	CCE (%)	Gypsum (%)	Anhydrite (%)	OC (%)	SAR (mmol L^{-1})$^{0.5}$
A	0-15	91.4	3.0	5.6	40	8.1	0.5	4.0	ng	ng	0.5	1.0
C1	15-45	95.4	1.0	3.6	50	8.2	0.3	0.5	ng	ng	0.3	0.3
C2	45-75	96.4	1.0	2.6	51	8.2	0.3	6.5	ng	ng	0.1	0.2
C3	75-110	97.4	1.0	1.6	53	8.2	0.3	4.0	ng	ng	0.1	0.2
C4	110-145	97.1	1.0	1.9	74	7.9	0.3	3.7	ng	ng	ng	0.2

Pedon 11, Alluvial fan, 680 m a.s.l., old alluvial fan, USDA: Typic Calciargids

Horizon	Depth (Cm)	Sand (%)	Silt (%)	Clay (%)	RF (%)	pH	ECe (dS m^{-1})	CCE (%)	Gypsum (%)	Anhydrite (%)	OC (%)	SAR (mmol L^{-1})$^{0.5}$
A	0-30	39.8	24.0	36.2	50	8.0	0.6	8.7	0.1	ng	0.2	4.2
Btk	30-70	29.8	22.0	48.2	48	7.7	0.5	15.5	0.1	ng	0.1	7.9
Bk	70-110	75.8	14.0	10.2	60	8.1	0.7	18.0	0.2	ng	0.1	7.2
C	110-150	87.8	4.0	8.2	69	7.9	0.9	22.7	0.1	ng	0.7	6.1

Pedon 12, Alluvial fan, 635 m a.s.l., old Alluvial fan, USDA: Typic Haplocalcids

Horizon	Depth (Cm)	Sand (%)	Silt (%)	Clay (%)	RF (%)	pH	ECe (dS m^{-1})	CCE (%)	Gypsum (%)	Anhydrite (%)	OC (%)	SAR (mmol L^{-1})$^{0.5}$
A	0-30	72.4	18.6	9.0	5	8.2	0.7	9.0	ng	ng	0.1	4.6
Bk	30-55	78.4	12.6	9.0	38	7.7	3.1	12.7	ng	ng	0.2	7.5
C1	55-85	80.4	8.6	11.0	53	7.7	3.9	10.5	ng	ng	0.1	8.7
C2	85-110	88.4	2.6	9.0	72	8.0	2.3	11.7	ng	ng	0.2	8.1
C3	110-135	82.4	6.6	11.0	58	8.0	2.6	11.7	ng	ng	0.2	9.7
C4	135-165	62.4	12.6	25.0	83	8.1	2.2	11.7	ng	ng	0.1	14.4

Pedon 13, Alluvial fan, 632 m a.s.l., young Alluvial fan, USDA: Typic Torrifluvents

Horizon	Depth (Cm)	Sand (%)	Silt (%)	Clay (%)	RF (%)	pH	ECe (dS m^{-1})	CCE (%)	Gypsum (%)	Anhydrite (%)	OC (%)	SAR (mmol L^{-1})$^{0.5}$
A	0-5	80.4	10.6	9.0	51	7.7	0.8	9.0	ng	ng	0.1	0.8
C1	5-25	80.4	12.6	7.0	56	8.1	0.5	12.2	ng	ng	0.1	1.5
C2	25-40	86.4	4.6	9.0	64	8.1	0.5	12.5	ng	ng	0.1	0.9
C3	40-70	82.4	6.6	11.0	62	7.9	0.6	12	ng	ng	0.1	1.5
C4	70-90	68.4	14.6	17.0	77	7.8	0.8	12.5	ng	ng	0.2	3.2
C5	90-130	58.4	22.6	19.0	66	7.8	0.9	11.7	ng	ng	0.2	4.1

Pedon 14, Rock pediment, 793 m a.s.l., limestone, USDA: Typic Gypsiargids

Horizon	Depth (Cm)	Sand (%)	Silt (%)	Clay (%)	RF (%)	pH	ECe (dS m⁻¹)	CCE (%)	Gypsum (%)	Anhydrite (%)	OC (%)	SAR (mmol L⁻¹)^0.5
A	0-40	56.4	34.6	9.0	54	7.8	1.0	19.2	ng	ng	0.1	0.7
Btk1	40-80	50.4	34.6	15.0	43	7.8	0.8	20.0	ng	ng	0.2	1.2
Btk2	80-105	46.4	36.6	17.0	27	7.8	1.8	15.2	ng	ng	0.1	3.9
C	105-110	56.4	28.6	15.0	55	7.8	2.1	16.5	ng	ng	0.1	3.4
2Btk	110-125	48.4	36.6	15.0	4	7.6	3.6	21.0	0.1	ng	0.1	4.1
2Bty	125-150	43.0	38.3	18.7	3	7.6	3.5	10.7	24.0	ng	0.1	3.8
2Cy	150-170	64.5	25.3	10.2	53	7.7	3.8	14.0	17.6	ng	0.1	5.3
Pedon 15, Playa (sodic clay flat), 368 m a.s.l., Playa deposits, USDA: Typic Haplosalids												
Az	0-15	3.7	60.5	35.8	0	7.3	202.0	12.7	1.1	ng	0.7	359.9
Btnz	15-35	0.0	46.2	53.8	0	7.0	108.1	13.2	0.6	ng	0.4	117.5
C	35-50	0.0	84.2	15.8	0	7.2	60.2	17.5	0.2	ng	0.2	62.0
2Bz1	50-75	1.7	68.5	29.8	0	7.1	87.4	16.2	0.4	ng	0.2	121.2
2Bz2	75-110	13.7	60.5	25.8	0	7.5	58.1	16.5	0.3	ng	0.2	130.2
2Cz	110-145	9.7	78.5	11.8	0	7.9	24.5	18.2	ng	ng	0.1	111.9

Horizon	Depth (Cm)	Sand (%)	Silt (%)	Clay (%)	RF (%)	pH	ECe (dS m⁻¹)	CCE (%)	Gypsum (%)	Anhydrite (%)	OC (%)	SAR (mmol L⁻¹)^0.5
Pedon 16, Playa (clay flat), 364 m a.s.l., Playa deposits, USDA: Typic Torriorthents												
A	0-20	8.4	64.6	27.0	0	8.3	3.2	16.2	ng	ng	0.3	67.8
C	20-60	20.4	70.6	9.0	0	7.7	11.1	16.5	ng	ng	0.1	46.8
2Cz	60-90	0.0	76.2	23.8	0	7.6	23.6	16.7	ng	ng	0.2	71.6
3Btnzb1	90-120	1.7	50.0	48.3	0	7.6	27.2	14.7	2.8	ng	0.2	77.3
3Btnzb2	120-150	9.7	42.5	47.8	0	7.7	32.1	14.0	3.1	ng	0.2	104.2
Pedon 17, Playa (fan delta), 378 m a.s.l., Playa deposits, USDA: Typic Torrifluvents												
A	0-20	32.4	46.6	21.0	0	7.5	1.8	13.0	ng	ng	0.2	4.5
C1	20-55	62.4	26.6	11.0	0	7.9	0.5	14.0	ng	ng	0.1	3.8
C2	55-85	2.4	60.6	37.0	0	8.3	1.2	16.7	ng	ng	0.1	11.0
C3	85-130	28.4	54.6	17.0	0	8.5	1.3	16.2	ng	ng	0.1	20.0
C4	130-160	50.4	36.6	13.0	0	8.4	1.0	14.7	ng	ng	0.2	16.5
Pedon 18, Playa (wet zone), 370 m a.s.l., Playa deposits, USDA: Typic Aquisalids												
Az	0-15	2.4	74.6	23.0	0	7.3	78.2	15.0	0.4	ng	0.5	189.5
Bz	15-30	8.4	70.6	21.0	0	7.5	57.3	16.0	1.2	ng	0.4	120.4
Btnz1	30-45	8.4	60.6	31.0	0	7.5	57.1	15.5	1.3	ng	0.5	118.7
Btnz2	45-95	0.0	71.0	29.0	0	8.2	43.3	15.5	0.6	ng	0.4	179.3
Bzg1	95-125	6.4	68.6	25.0	0	8.4	32.7	15.7	0.6	ng	0.3	151.7
Bzg2	125-170	30.4	48.6	21.0	0	8.1	30.2	17.0	0.5	ng	0.3	77.7
Pedon 19, Playa (clay flat with puffy ground), 374 m a.s.l., Playa deposits, USDA: Typic Haplosalids												
Az	0-30	0.4	47.3	52.3	0	8.3	92.7	11.5	4.8	ng	0.2	813.1
Bz1	30-60	4.4	45.3	50.3	0	8.2	70.6	11.7	4.3	ng	0.2	506.2
Bz2	60-90	0.0	67.7	32.3	0	8.2	99.4	11.0	1.7	ng	0.3	730.8
Bz3	90-135	0.4	59.3	40.3	0	8.3	69.8	13.0	0.5	ng	0.3	512.5
Bz4	135-155	14.4	51.3	34.3	0	8.2	49.5	13.0	ng	ng	0.2	330.6
Pedon 20, Playa (salt crust), 367 m a.s.l., Playa deposits, USDA: Typic Haplosalids												
Az	0-30	3.8	64.6	31.6	0	8.1	222.2	17.2	2.2	ng	0.4	1631.7
Bz1	30-60	1.8	60.6	37.6	0	8.2	138.4	18.0	0.9	ng	0.2	609.2
Bz2	60-90	5.8	58.6	35.6	0	8.0	78.1	15.5	2.0	ng	0.3	367.0
Bz3	90-120	15.8	48.6	35.6	0	8.0	51.4	15.5	1.7	ng	0.1	360.2
Bz4	120-155	17.8	52.6	29.6	0	8.0	35.6	15.0	2.3	ng	0.1	170.0

174 ng: negligible, RF: rock fragment, ECe: electrical conductivity of soil saturated extract, OC: organic carbon, CCE:
175 calcium carbonate equivalent, a.s.l.: above sea level, SAR: sodium adsorption ratio

176

177

178

Table 2. Semi-quantitative mineralogical composition of clay minerals of soils and parent rocks in the studied area.

Landforms	Pedons	Parent materials	Soil moistures	Horizons	Smectite	Palygorskite	Illite	Chlorite	Kaolinite
Piedmont plain	1	Diorite	Xeric	Bw1	XXX	XX	XXX	ND	X
				R	XX	ND	XXXX	XX	X
Low land	2	Diorite	Aquic	Bg1	ND	ND	XXXXX	ND	XX
Mantel pediment	3	Andesite	Xeric	2Btk	XXXX	ND	XXX	ND	X
	4	Limestone	Aridic	Btk1	XX	XX	XXX	XXX	X
				2Ck	XX	XX	XXX	XX	X
	5	Diorite	Aridic	Btk	XXX	XX	XXXX	X	X
	6	Diorite	Aridic	Btn1	XXXXX	ND	XX	ND	X
				2Btk	XX	XX	XXXX	XX	X
	7	Diorite	Aridic	Bty	XXX	XX	XX	XX	X
	8	Andesite	Aridic	Bkyz1	XX	XX	XXX	XXX	X
	9	Diorite	Aridic	Btkyz	XXX	XX	XXX	XX	X
Rock pediment	14	Limestone	Aridic	Btk1	XX	XX	XXXX	ND	X
Playa	18	Playa deposit	Aquic	Bzn	XXX	XX	XXX	XX	X
				Btnz2	XXXX	ND	XXX	ND	X

Relative abundance of clay minerals is shown by: X: < 10 %; XX: 10-25 %; XXX: 25-50 %; XXXX: 50-75 %; XXXXX: > 75 %; ND: not detected.

3.3. Mantled pediment

Mantled pediment covers a vast area in the region. Soils in this landform were affected by igneous (pedons 3 and 8), diorite (pedons 5-7 and 9), and sedimentary limestone (pedon4) parent materials (Mohammadi, 2011) with two xeric and aridic soil moisture regimes. Argillic and calcic horizons were found in most pedons under study, but gypsic horizon was only found in the parts with an aridic soil moisture regime (Table 1). The argillic horizon (Fig. 2a) in the xeric parts of the area (pedon 3) could be due to the present humidity of the area, whereas argillic in other pedons with an aridic moisture regime, could only be attributed to the more available humidity of the past. Evidence of more humid paleoclimate in central Iran was reported by other researchers (Farpoor et al., 2012; Khormali et al., 2003; Khademi and Mermut, 2003).

Calcium carbonate equivalent (CCE) increased with depth (Table 1) in pedon 4 due to the presence of a calcareous parent material (about 89% in 2Ckk horizon). Besides, natric, salic, and

196 anhydritic horizons were also investigated in mantled pediment position. Anhydrite in pedons 7
197 and 8 was probably formed from dehydration of gypsum at the later stages of evaporation through
198 evolution of the landform. High temperature caused this mineral to be preserved (Sarmast et al.,
199 2017; Wilson et al., 2013).

200 Pedons 3 and 8 with the same parent material (andesite) showed different evolutions. Pedon 3 in
201 the xeric part of the area had an argillic horizon, whereas no argillic was found in aridic parts with
202 about 1800 m asl. Climate seems to be the only factor controlling soil evolution in these pedons.
203 Pedon 3 is an Alfisol, but the other pedons were classified as Aridisols (Table 1).

204 Micromorphological observations showed clay (pedons 3-7 and 9), calcium carbonate (pedons 3-
205 4 and 9), gypsum (pedons 5, 8-9), anhydrite (pedon 7), and compound (pedons 3 and 9) pedo-
206 features (Fig. 2). Clay coating in pedon 3 (Fig. 2a) with a xeric soil moisture regime was probably
207 formed in the present climatic conditions of the area. On the other hand, argillic horizon formation
208 and clay coatings (Figs. 2 b, e, g, i, l, m) in other pedons in this landform with an aridic soil moisture
209 regime could only be attributed to the presence of a more humid climate in the past. This was also
210 supported by Farpoor et al. (2012), Sanjari et al. (2011), and Kademi and Mermut (2003) in Sirjan
211 playa, Jiroft, and Isfahan arid areas of central Iran, respectively. A different clay coating in
212 2Btnkk1 horizon of pedon 4 was observed (Fig. 2c) which was affected by high Na content. This
213 type of clay coatings was reported for the natric horizons where dispersion was induced by Na. The
214 same results were also reported for saline and sodic soils of Fars Province by Khormali et al. (2003).

215 Calcite coatings were observed on the clay coatings in Btk horizon of pedon 3 (Fig. 2a) and Btky
216 horizon of pedon 9 (Fig. 3m). The mentioned order of coatings in pedon 3 could be formed at the
217 climatic situations of the present time, but for the pedon 9 is a proof of clay illuviation during more
218 available humidity of the past, followed by calcite illuviation along later aridity as was also
219 supported by Bayat et al. (2017) and Moghbeli et al. (2019). The compound clay-calcite pedo-
220 feature is a proof of the formation of a polygenetic soil which has experienced different formation-
221 development cycles due to climatic fluctuations.

222 Calcite coatings (Figs. 2a, d, m, o) are among the most important pedo-features which have
223 formed through re-precipitation of illuviated calcium carbonates originated from upper horizons
224 (Kemp et al., 2003). Dissolved calcium carbonate in the arid climate of the present time has formed
225 infillings (Fig. 2d, o) in the pore spaces (Durand et al., 2010). Sarmast et al. (2019) reported coating,
226 infilling and nodule pedo-features of calcite in soils of central Iran.

227   Meanwhile, lenticular and interlocked plates of gypsum (Fig. 2f) in By horizon of pedon 5 on

228   mantled pediment were investigated. Soils of this pedon were not saline (Table 1) and were

229   composed of high sand and coarse gravel contents. Large pore space content of the soil could

230   facilitate lenticular formation of gypsum as was also supported by Amit and Yaloon (1996) and

231   Farpoor et al. (2012) in Israel and central Iran, respectively. The same mechanism could also be

232   attributed to the lenticular gypsum formation in Btky horizon of pedon 9 (Fig. 2k). Gypsum

233   pendants (macroscopic form) and gypsum interlocked plates (microscopic form) in pedons 5 and

234   8 were attributed to coarse texture and high gravel content of pediments (Farpoor et al., 2003).

235   Meanwhile, anhydrite was also formed in By1 horizon of pedon 7 (Fig. 2h), seemingly during

236   gypsum transformation. The same results were reported by Aref (2003) and Sarmast et al. (2019)

237   in soils of Egypt and central Iran, respectively.

238   Smectite, illite, and kaolinite clay minerals were found in pedon 3 (Table 2, Fig. 3d). Palygorskite

239   and chlorite could not be formed or have been weathered in this position due to a xeric moisture

240   regime. Smectite is the dominant clay mineral in this pedon (Table 2). Moreover, smectite, illite,

241   chlorite, kaolinite, and palygorskite were found in soil (Btk1) and parent material (2Ck) of pedon

242   4 (Table 2. And Figs. 3e, f). The presence of the above-mentioned minerals in soils and parent

243   material is a proof of inheritance origin from sedimentary formations which was also supported by

244   Owliaie et al. (2018) for soils located on sedimentary formations of southwest Iran.

245   On the other hand, smectite, illite, chlorite, palygorskite, and kaolinite clay minerals were

246   identified in other pedons (5-9) on this landform which were affected by igneous formations (Table

247   2, Figs. 3 g, h, i, j, k, l). No palygorskite was found in the igneous parent material (Fig. 2b), but

248   calcic (Fig. 3i) and gypsic (Fig. 3j) horizons contained palygorskite. Geochemical conditions after

249   the precipitation of calcium as calcium carbonate and gypsum in the arid climate of these pedons

250   seem to have been favorable for palygorskite formation together with the increase of soluble Mg

251   (Singer and Fine, 1989). A pedogenic origin for palygorskite in calcic (2Btk) horizon of pedon 6

252   (Fig. 4a) and gypsic horizon (Bty) of pedon 7 (Fig. 4b), both affected by igneous formations was

253   proved using electron microscope observations. Preservation of palygorskite around calcite

254   (Khademi and Mermut, 1998) and gypsum (Owliaie et al., 2018; Moazallahi and Farpoor, 2012;

255   Khademi and Mermut, 1998) crystals in soils and sediments of central Iran were also reported.

256   Moreover, the lack of palygorskite and chlorite in the modern topsoil of pedon 6 (Fig. 3h) could be

257   attributed to the Halilrood River floods which may have caused their transformation to smectite

258 (Birkland, 1999). Smectite is the dominant mineral in the modern topsoil of pedon 6 (Table 2)

259 which is another support for the above-mentioned discussion. Thus, both pedogenic and inherited

260 origins for smectite in soils of the area are plausible (Sanjari et al., 2011).
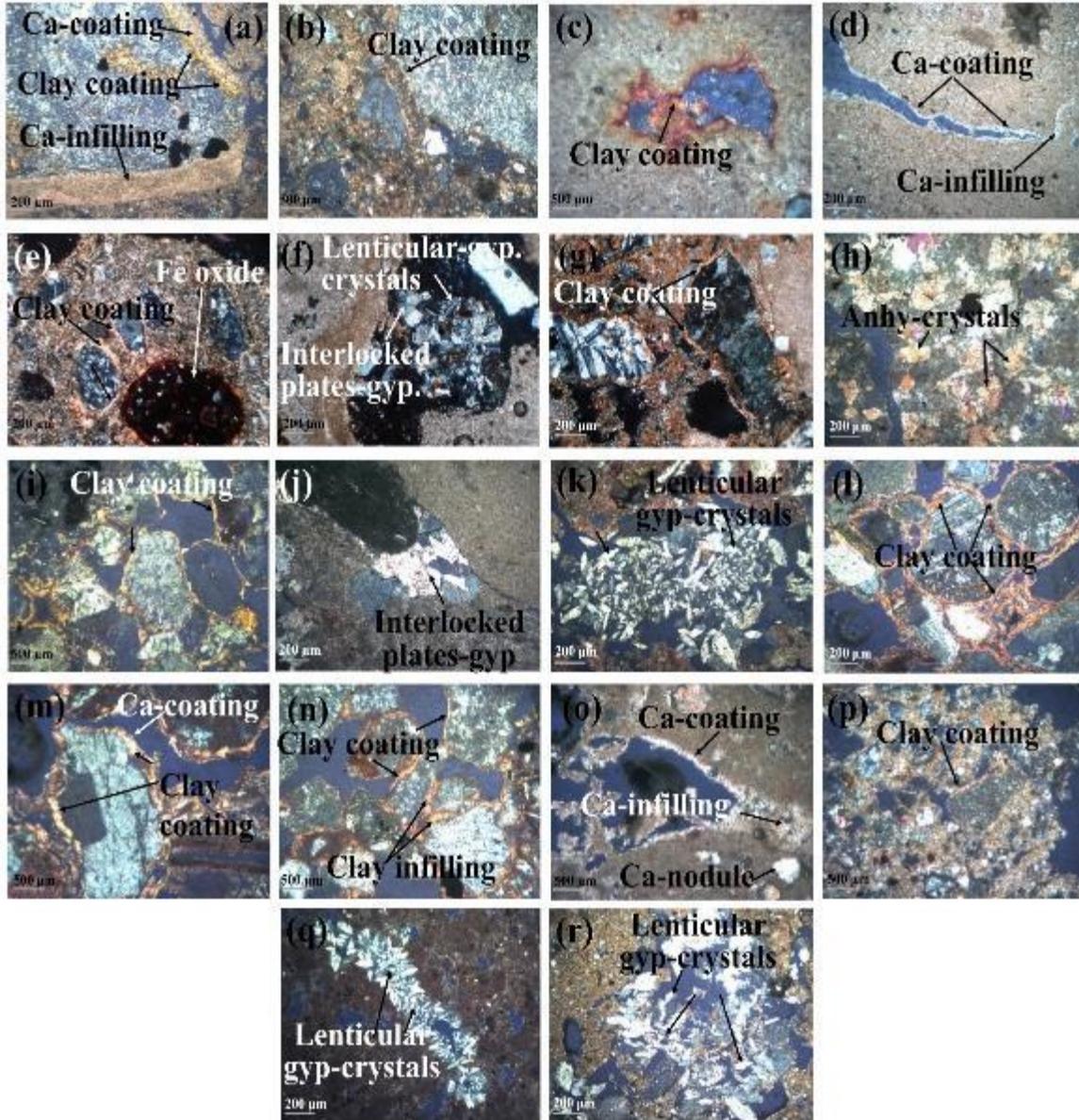
261

262 **Figure 2.** Thin sections of a) Clay and calcite coatings and dense incomplete calcite infilling in Btk horizon, pedon 3
263 (XPL), b) Clay coating in Btk2 horizon, pedon 4 (XPL), c) Clay coating in 2Btnkk1 horizon, pedon 4 (XPL), d) Coating
264 and infilling of calcite in 2Btnkk1 horizon, pedon 4 (XPL), e) Clay coating and Fe oxide in Btk horizon, pedon 5
265 (XPL), f) Interlocked plates and lenticular forms of gypsum crystals in By horizon, pedon 5 (XPL), g) Clay coating in
266 2Btk horizon, pedon 6 (XPL),), h) Anhydrite crystals in By1 horizon, pedon 7 (XPL), i) Clay coating in Bty horizon,
267 pedon 7 (XPL), j) Interlocked plates of gypsum in Bkyzn horizon, pedon 8 (XPL), k) Lenticular gypsum crystals in
268 Btky horizon, pedon 9 (XPL), l) Clay coating in Btky horizon, pedon 9 (XPL), m) Clay and calcite coating in Btky
269 horizon, pedon 9 (XPL), n) Coating and infilling of clay in Bk horizon, pedon 11 (XPL), o) Calcite coating, infilling,
270 and nodule in Bk horizon, pedon 12 (XPL), p) Clay coating in Btk1 horizon, pedon 14 (XPL), q) Lenticular gypsum
271 crystals in 3Btnzb1 horizon, pedon 16 (XPL), r) Lenticular gypsum crystals in Bz2 horizon, pedon 20 (XPL).

Figure 3. X-Ray diffractograms of the clay fraction, a) Bw1 horizon of pedon 1. b) R horizon of pedon 1, c) Bg1 horizon of pedon 2, d) 2Btk horizon of pedon 3, e) Btk1 horizon of pedon 4, f) 2Ck horizon of pedon 4, g) Btk horizon of pedon 5, h) Btn1 horizon of pedon 6, i) 2Btk horizon of pedon 6, j) Bty horizon of pedon 7, k) Bkyz1 horizon of pedon 8, l) Btky horizon of pedon 9, m) Btk1 horizon of pedon 14, n) Bz horizon of pedon 18, o) Btnz2 horizon of pedon 18. (Sm: Smectite, I: Illite, Pa: Palygorskite, Ch:Chlorite, Ka:Kaolinite. Mg=Mg saturated; Mg-Eg=Mg saturated with Ethylene glycol; K=K saturated; K-550=K saturated and heated to 550 °C).

304   Pedons 3 and 8 with the same parent material and geomorphology, but different soil moisture

305   regime, have different soils. This is a proof for the important role of climate in soil formation

306   compared to p (parent material) and r (relief) as soil forming factors in this part of the area. On the

307   other hand, pedons 4 to 9 have the same geomorphology and climate, but parent material for pedon

308   4 (limestone) is different with other pedons (diorite). Results clearly show that somehow similar

309   soils were formed in these pedons and limited differences in the suborder level were only observed.

310   This in turn shows the high effective role of climate and geomorphology on soil formation in this

311   landform.

312

3.4. Alluvial fan

314   Similar to mantled pediment, soils with various evolution were found in this landform. Soil

315   moisture regime for alluvial fan is aridic which is why different soil evolutions (pedons 10-13)

316   could be due to the difference in parent material (Table 1). Pedons 10 (east of Jiroft) and 13 (east

317   of Iranshahr) located on young alluvial fan deposits and affected by granite formations showed

318   very little soil development. The large distance from Neogene gypsiferous and saline formations

319   on one hand, and the young Quaternary alluvial fan deposits on the other hand, are among the

320   inhibiting factors controlling soil development in this geomorphic position. Moreover, the

321   formation of bajada due to rainfall and the erosion of upland mountains in these two locations

322   which are in the arid zone climate, could be evidence of a more humid climate in the past. The

323   same results were also reported by Sarmast et al. (2017) in the study of alluvial fans in the central

324   parts of Iran. Pedons 11 (with argillic and calcic horizons) and 12 (with calcic horizon) respectively

325   affected by limestone and diabase (influenced by Mokran colored melange) parent materials

326   showed soils with high and intermediate evolution located on old alluvial fan deposits.

327   Micromorphological observations showed clay coatings and infillings in Btk horizon of pedon 11

328   (Fig. 2n) which are supporting proofs of argillic horizon formation. Calcite coating, infilling, and

329   nodules were also determined in Bk horizon of pedon 12 (Fig. 2o). Formation of calcite nodule

330   (Fig. 2o) in the Btk horizon of pedon 12 was due to dissolution/recrystallization of calcite in the

331   groundmass. Sarmast et al. (2019) reported coating, infilling and nodule pedo-features of calcite in

332   soils of central Iran. Entisols and Aridisols were formed on this geomorphic position.

333   Pedons 10 to 13 have the same geomorphology (alluvial fan) and climate (aridic soil moisture

334   regime), but different parent material (igneous in pedons 10 and 13 vs. sedimentary in pedons 11

335 and 12). Formation of different soils is a proof of the role of parent material and time on soil

336 formation when other soil formation factors are the same.

337

338 ### 3.5. Rock pediment

339 This geomorphic position about 800 m asl and with an aridic soil moisture regime is affected by

340 limestone together with shale and marl as parent material. Pedon 14 with argillic, calcic, and gypsic

341 horizons were described and sampled on this position. Due to low SAR content (Table 1) and an

342 aridic soil moisture regime, presence of argillic horizon similar to other arid parts of Jazmurian

343 Watershed was attributed to the more available humidity of the past. That is why this soil was

344 accounted as a paleosol. Removal of calcium carbonate from upper horizons with more humidity

345 of the past (Bk horizon formation) followed by clay illuviation caused Btk horizon to be formed

346 (Sanjari et al., 2011). Clay coating proved illuviation of clay and argillic horizon formation (Fig.

347 2p). Clay mineralogy of this soil was similar to mantled pediment position (Table 2, Fig. 3m). This

348 soil was classified as Typic Calcigypsids.

349

350 ### 3.6. Playa

351 Sodic clay flat (pedon 15), clay flat (pedon 16), fan delta (pedon 17), wet zone (pedon 18), puffy

352 ground clay flat (pedon 19), and salt crust (pedon 20) geomorphic surfaces were found in playa

353 about 360 m asl (Fig. 1). Salic and natric were the dominant horizons found in soils of this

354 landform. High Na content caused clay dispersion and natric horizon formation in some pedons of

355 this position as was also supported by Khormali et al. (2003). A modern and a buried paleosol were

356 found (pedon 16) on clay flat geomorphic position. The modern soil with A and C horizons was a

357 young soil affected by alluvial deposits, and 2Cz horizon showed the influence of aeolian deposits.

358 Active wind erosion of the upland positions caused wind-blown deposits in this horizon. On the

359 other hand, the buried soil is a developed soil with salic and natric horizons. Meanwhile, a non-

360 saline (Table 1) Fluvisol (pedon 17) was found on fan delta geomorphic surface. Formation

361 processes of fan delta position and the role of Halilrood River with a non-saline water, could be

362 accounted for a non-saline soil to be formed in pedon 17.

363 Wet zone with an aquic soil moisture regime was located between alluvial fan and clay flat

364 positions. The same geomorphic position was also reported by Farpoor et al. (2012) in Sirjan Playa.

365 High electrical conductivity (EC) in the topsoil of puffy ground clay flat was attributed to

366 evaporation and capillary water movement in this geomorphic position (Sanjari et al., 2011). The

367   thickness of salt polygons in the salt crust geomorphic position of the area was less than what

368   reported for other playas (Sirjan, and Lut) of central Iran. Bampour seasonal river which has passed

369   through evaporate formation of east side watershed contains more soluble salts compared to non-

370   saline Halilrood River. Salt crust seems to be affected by Bampour River. Soils of this position

371   were classified as Entisols and Aridisols (Table 1).

372   Lenticular gypsum crystals observed in 3Btnzb1 (pedon 16) and Bz2 (pedon 20) horizons. Soils

373   in this position were fine textured with small pore spaces and high salinity (Table 1). The reason

374   could be attributed to the NaCl content (Amit and Yaloon 1996) together with super saturation in

375   respect to calcium sulfate in the fine pore spaces along time periods (Owliaie et al. 2006). Since

376   gypsum content was not enough, gypsic horizon was not detected in these pedons.

377   Palygorskite was not detected in Btnz2 horizon of pedon 18 on wet zone geomorphic position

378   (Fig. 3o). Due to high humidity content in this position (presence of an aquic soil moisture regime),

379   transformation of palygorskite to smectite which was also reported by Khormali and Abtahi (2003)

380   and Moghbeli et al. (2019) could not be neglected in this position. The dominance of smectite in

381   this soil (Table 2) could be another support for the above-mentioned discussion. Since smectite

382   was also determined (Fig. 3n) in the Bz horizon (near the soil surface), it seems that the detrital

383   origin of smectite addition to the surface could be another plausible reason. The intense 0.63 nm

384   peak of palygorskite was also due to the detrital transportation of broken palygorskite crystals from

385   alluvial fan toward this position. That is why palygorskite in this geomorphic position is with a

386   detrital origin which was also supported by split crystals observed using electron microscopy (Fig.

387   4). Farpoor and Irannejad (2013) and Khademi and Mermut (1998) also came to the same

388   conclusion in Rafsanjan and Isfahan areas, central Iran.

389   Parent material and climate for pedons 15 to 20 are the same, but geomorphic surfaces have only

390   changed which caused differences in order and suborder levels of soils formed in playa. This shows

391   the role of topography (r) apart from climate and parent material in soil formation.

392

393

394
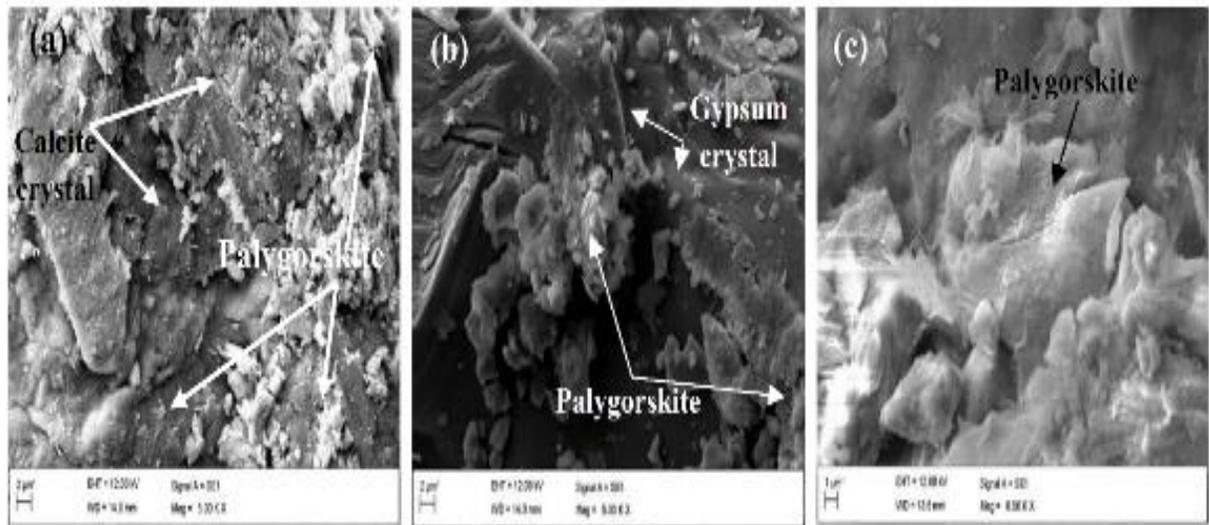
Figure 4. SEM micrographs of (a) palygorskite fibers on calcite crystal of the 2Btk horizon of pedon 4, (b) palygorskite fibers on gypsum crystal of the Bty horizon of pedon 5, (c) palygorskite broken fibers of the Bzn horizon of pedon 18.

4. Conclusions

Various soils were formed through the climolithotoposequence studied in Jazmurian Watershed. The electrical conductivity content increased toward playa and the maximum EC content of 222.2 dS/m was determined in salt crust geomorphic position of playa. Soil evolution was highly depended on parent material and the decreasing trend of soil evolution (granite-young alluvial fan deposits< playa deposits< limestone-old alluvial fan deposits< andesite- diorite) was found in the area. Soils were classified as Mollisols, Alfisols, Aridisols, Inceptisols, and Entisols. Different pedofeatures in argillic and calcic horizons in both xeric and aridic soil moisture regimes of the area were found. However, pedo-features related to gypsic and anhydritic horizons were only found in the arid parts of the transect. The presence of a more humid paleoclimate in the history of the area which was supported by clay coatings was proved by argillic horizons formed in the arid parts of the area. A dispersed clay coating was found in natric horizons. Smectite, illite, chlorite, palygorskite, and kaolinite clay minerals were identified. Palygorskite was only found in the arid parts of the area and pedogenic and inherited origins were respectively found in igneous and sedimentary affected soils. Palygorskite in piedmont plain about 3620 m asl was with an aeolian origin. Illite and chlorite clay minerals were identified in both sedimentary and igneous parent materials with an inherited origin, but lack of these minerals in some of the soils under study could be attributed to their transformation to smectite which was also supported by smectite peak

416   intensity in such soils. That is why both inherited and transformed (from illite, chlorite, and

417   palygorskite) sources of smectite in the area were plausible.

418   Results of the study emphasized on the more effective role of climate and relief on soil formation

419   compared to parent material. The role of climate, alone or together with relief on soil formation

420   and evolution in pedons 1 to 9 seems to be greater than that of parent material. Since climate and

421   relief have not changed along pedons 10 to 14, parent material affected soil formation and

422   evolution. Moreover, relief has controlled soil formation and development in pedons 15 to 20 as

423   climate and parent material were the same in these pedons. The hypothesis regarding the effects of

424   climate, topography, and parent material soil forming factors on soil formation and development

425   (climolithotoposequence) in the area was clearly proved.

426

427   **References**

428   Amit. R., Yaalon, A. D., 1996. The micromorphology of gypsum and halite in reg soils: The

429   Negev desert, Israel. Earth Surf. Proc. Landf. 21, 1127–1143.

430   Aref, M. A. M., 2003. Classification and depositional environments of Quaternary pedogenic

431   gypsum crusts (gypcrete) from east of the Fayum Depression, Egypt. Sed. Geol. 155(1), 87–108.

432   Artieda, O., Herrero, J., Drohan, P. J., 2006. Refinement of the differential water loss method for

433   gypsum determination in soils. Soil Sci. Soc. of Amer. J. 70, 1932–1935.

434   Badia, D., Buendia-Garcia, L., Longares-Aladrén, L., Marti-Dalmau, C., Peña-Monné, J.,

435   González-Pérez, J., Gómez-Garcia, D., 2020. Soil-geomorphology relationships determine the

436   distribution of the main subalpine grasslands in the Central Pyrenees (NE-Spain). Sci. of the Total

437   Environ. 734, 139121.

438   Banaie, M. H., 1998. Soil Moisture and Temperature Regimes Map of Iran. Iran: Soil and Water

439   Res. Institute.

440   Bayat, O., Karimzadeh, H., Karimi, A., Karimian Eghbal, M., Khademi, H., 2017.

441   Paleoenvironment of geomorphic surfaces of an alluvial fan in the eastern Isfahan, Iran, in the light

442   of micromorphology and clay mineralogy. Arab. J. of Geosci. 10, 91

443   Birkeland, P. W., 1999. Soils and Geomorphology. New York: Oxford University Press.

444   Bower, C. A., Hatcher, J. T., 1966. Simultaneous determination of surface area and cation

445   exchange capacity. Soil Sci. Soc. of Amer. J. 30, 525–527.

446 Durand, N., Monger, H. C., Canti, M. G., 2010. Calcium carbonate features. In: G. Stoops, V.
447 Marcelino, & F. Mees (Eds.), Interpretation of micromorphological features of soils and regoliths.
448 Amsterdam, Netherlands (pp. 149–182). Elsevier.

449 Egli, M., Merkli Ch., Sartori, G., Mirabella, A., Plotze, M., 2008. Weathering, mineralogical
450 evolution and soil organic matter along a Holocene soil toposequence developed on carbonate-rich
451 materials. Geomorphology 97, 675–696.

452 Elliott, P.E., Dorhan, P.J., 2009. Clay accumulation and argillic-horizon development as
453 influenced by aeolian vs. local parent material on quartzite and limestone-derived alluvial fans.
454 Geoderma 151, 98-108.

455 Farpoor, M. H., Eghbal, M. K., Khademi, H., 2003. Genesis and micromorphology of saline and
456 gypsiferous Aridisols on different geomorphic surfaces in Nough area, Rafsanjan. J. of Sci. & Tech.
457 of Agri. & Natur. Resour. 7, 71–93. (in Persian with English abstract)

458 Farpoor, M. H., Neyestani, M., Eghbal, M. K., Esfandiarpour Borujeni, I., 2012. Soil–
459 geomorphology relationships in Sirjan playa, south-central Iran. Geomorphology 138(1), 223–230.

460 Farpoor, M. H., Irannejad, M., 2013. Soil genesis and clay mineralogy on Aliabbas River alluvial
461 fan, Kerman Province. Arab. J. of Geosci. 6(3), 921–928.

462 Gee, G. W., Bauder, J. W., 1986. Particle size analysis. In: A. Klute (Eds.), Methods of Soil
463 Analysis, Agronomy Monograph, Vol 9 (pp. 383–411). Madison, WI: American Society of
464 Agronomy/Soil Science Society of America.

465 Graham R.C., O'Geen A.T., 2010. Soil mineralogy trends in California landscapes. Geoderma
466 154, 418–437.

467 Jackson, M. L., 1975. Soil Chemical Analysis-advanced Course. Madison, WI: University of
468 Wisconsin College of Agriculture, Department of Soil Science.

469 Johns, W.D., Grim, R.E., Bradly, W.F., 1954. Quantitative Estimation of Clay Minerals by
470 Diffraction Methods. J. Sed. Petrol. 24, 242-251.

471 Kemp, R. A., Tomas, P. S., Sayago, J. M., Debyshire, E., King, M., Wagner, L., 2003.
472 Micromorphology OSL dating of the basalt part of the loess-paleosol sequence at La Mesuda in
473 Tucuman province, northwest Argentina. Quarter. Int. 106–107, 111–117.

474 Kittrick, J. A., Hope, E. W., 1963. A procedure for the particle-size separation of soils for X-ray
475 diffraction analysis. Soil Sci. *96(5)*, 319–325.

476   Khademi, H., Mermut, A. R., 1998. Source of palygorskite in gypsiferous Aridisols and
477   associated sediments from central Iran. Clay Miner. 33(4), 561–578.

478   Khademi, H., Mermut, A. R., 2003. Micromorphology and classification of Argids and associated
479   gypsiferous Aridisols from central Iran. Catena 54, 439–455.

480   Khormali, F., Abtahi, A., 2003. Origin and distribution of clay minerals in calcareous arid and
481   semiarid soils of Fars Province, southern Iran. Clay Miner. 38(4), 511–527.

482   Khormali, F., Abtahi, A., Mahmoodi, S., Stoops, G., 2003. Argillic horizon development in
483   calcareous soils of arid and semiarid regions of southern Iran. Catena 53(3), 273–301.

484   Krinsley, D. B., 1970. A Geomorphological and Paleoclimatological Study of the Playas of Iran.
485   Washington DC: Geological Survey, United States Department of Interior.

486   Moazallahi, M., Farpoor, M. H., 2012. Soil genesis and clay mineralogy along the xeric aridic
487   climotoposequence, South central Iran. J. of Agri. Sci. and Tech. 14, 683–696.

488   Moghbeli, M., Owliaie, H. R., Sanjari, S., Adhami, E., 2019. Genetic Study of Soil-Landscape
489   Relationship in Arid Region of Faryab, Kerman Province. J. of Water and Soil 33(2), 333–347. (in
490   Persian with English abstract)

491   Mohammadi, A., 2011. Sedimentology and sedimentary geochemistry of Jazmuriyan Playa. Arid
492   Biom Scientific and Res. J. 1(1): 68–78. (in Persian with English abstract)

493   Monafi, S.H. (2010). Mineralogical Evidence of Climate Change in some Semiarid Soils of
494   SouthernUrmia, Iran. Soil Science Agrochem. and Ecol. 4, 17-24.

495   Namaki, L., 2003. Analysis of Makran aeromagnetic data. Iran: University of Tehran, Institute of
496   Geophysics. (in Persian with English abstract)

497   Nelson, R. E., 1982. Carbonate and Gypsum. In: A. L. Page, R. H. Miller, & D. R. Keeney (Eds.),
498   Methods of Soil Analysis. Part II. 2nd ed., Agronomy Monogarph, Vol 9. Madison, WI: American
499   Society of Agronomy/Soil Science Society of America (pp. 181–196).

500   Nelson, D. W., Sommers, L. E., 1982. Total Carbon, Organic Carbon and Organic Matter. In: A.
501   L. Page, R. H. Miller, & D. R. Keeney (Eds.), Methods of Soil Analysis. Part II. 2nd ed., Agronomy
502   Monogarph, Vol 9. Madison, WI: American Society of Agronomy/Soil Science Society of America
503   (pp. 539–577).

504   O'Geen, A.T., Hobson, W.A., Dahlgren, R.A., Kelly, D.B., 2008. Evaluations of soil properties
505   and hydric soil indicators for vernal pool catenas in California. Soil Sci. Soc. of Amer. J. 72: 727–
506   740.

507   Owliaie, H. R., Abtahi, A., Heck, R. J., 2006. Pedogenesis and clay mineralogical investigation

508   of soils formed on gypsiferous and calcareous materials on a transect, Southwestern Iran.

509   Geoderma 134, 62–81.

510   Owliaie, H. R., Adhami, E., Najafi Ghiri, M., Shakeri, S., 2018. Pedological Investigation of a

511   Litho-Toposequence in a Semi-Arid Region of Southwestern Iran. Euras. Soil Sci. 51(12), 1447–

512   1461.

513   Paquet, H., Millot, C., 1972. Geochemical evolution of clay minerals in the weathered products

514   and soils of Mediterranean climates. Proceedings of the 9th International Clay Conference, Madrid,

515   Spain (pp. 199–202).

516   Phillips, J., Turkingtan, A.V., Marine, D.A., 2008. Weathering and vegetation affection early

517   stages of soil formation. Catena 72, 21-28.

518   Saez, A., Ingles, M., Cabrera, L., Heras, A., 2003. Tectonic Paleoenvironmental Forcing of Clay-

519   Mineral Assemblages in Non-Marine Setting: The Oligocene-Miocene Aspontes Basin (Spain).

520   Sed. Geol. 159: 305-324.

521   Sanjari, S., Farpoor, M. H., Eghbal, M. K., Esfandiarpoor Boroujeni, I., 2011. Genesis,

522   micromorphology and clay mineralogy of soils located on different geomorphic surfaces in Jiroft

523   area. J. of Water and Soil 25(2), 411–425. (in Persian with English abstract)

524   Sanjari, S., Farpoor, M. H., Esfandiarpoor Boroujeni, I., Eghbal, M. K., 2012. Micromorphology

525   and clay mineralogy comparison of past and present soils in Jiroft area. J. of Water and Soil Sci.

526   15(58): 173-185 (in Persian with English abstract).

527   Sarmast, M., Farpoor, M. H., Esfandiarpour Boroujeni, I., 2017. Soil and desert varnish

528   development as indicators of landform evolution in central Iranian deserts. Catena 149, 98–109.

529   Sarmast, M., Farpoora, M. H., Jafaria, A., Esfandiarpour Borujeni, I., 2019. Tracing

530   environmental changes and paleoclimate using the micromorphology of soils and desert varnish in

531   central Iran. Desert 24(2), 331–353.

532   Schoeneberger, P. J., Wysocki, D. A., Benham, E. C., 2012. Field Book for Describing and

533   Sampling Soils. Lincoln, NE: Natural Resources Conservation Service, National Soil Survey

534   Center.

535   Singer, A. (1989). Palygorskite and Sepiolite Group Minerals. In J.B. Dixon, & D.G. Schulze

536   (Eds.), Soil Mineralogy with Environmental Applications (pp. 556-580). Madison, Wisconsin,

537   USA: Soil Science Society of America.

538   Singer, M.J., Fine, P., 1989. Pedogenic factors affecting magnetic susceptibility of California

539   soils. Soil Sci. Soc. of Amer. J. 53, 1119-1127.

540   Soil Survey Staff, 2022. Keys to Soil Taxonomy, 13th Edition. Washington, D.C: United States

541   Department of Agriculture and Natural Resources Conservation Service.

542   Stoops, G., 2003. Guidelines for the Analysis and Description of Soil and Regolith Thin Sections.

543   Madison, WI: Soil Science Society of America.

544   Wilson, M. A., Shahid, S. A., Abdelfattah, M. A., Kelley, J. A., Thomas, J. E., 2013. Anhydrite

545   formation on the Coastal Sabkha of Abu Dhabi, United Arab Emirates. In: S. A. Shahid, F. K.

546   Taha, & M. A. Abdelfattah (Eds.). Developments in Soil Classification, Land Use Planning and

547   Policy Implications: Innovative Thinking of Soil Inventory for Land Use Planning and

548   Management of Land Resources (pp. 175–201). Netherlands: Springer SBM Publishing.

549   Wilson, S.G., Lambert, J.-J., Nanzyo, M., Dahlgren, R.A., 2017. Soil genesis and mineralogy

550   across   a   volcanic   lithosequence.   Geoderma   285,   301–312.   https://linkinghub.

551   elsevier.com/retrieve/pii/S001670611630430X.

552   Yousefifard, M., Ayoubi, S., Poch, R.M., Jalalian, A., Khademi, H., Khormali, F., 2015. Clay

553   transformation and pedogenic calcite formation on a lithosequence of igneous rocks in

554   northwestern Iran. Catena 133, 186–197.

555